Near-infrared sensitivity enhancement of silicon image sensor with wide incident angle

Atsushi Ono
Graduate School of Integrated Science and Technology, Shizuoka University
Research Institute of Electronics, Shizuoka University
Hamamatsu, Japan
ono.atsushi@shizuoka.ac.jp

Takahito Yoshinaga
Graduate School of Integrated Science and Technology, Shizuoka University
Hamamatsu, Japan
yoshinaga.takahito.17@shizuoka.ac.jp

Kazuma Hashimoto
Graduate School of Integrated Science and Technology, Shizuoka University
Hamamatsu, Japan
hashimoto.kazuma.15@shizuoka.ac.jp

Nobukazu Teranishi
Research Institute of Electronics, Shizuoka University
Hamamatsu, Japan
teranishi@idl.rie.shizuoka.ac.jp

***Abstract*—We proposed silicon-based image sensor with metal gratings and metal-filled deep trench isolation which improved near-infrared (NIR) sensitivity by plasmonic diffraction. The absorption efficiency was improved to 53% at an NIR wavelength 940 nm with 3-µm thick of silicon. Although, it has severe incident angle dependence of sensitivity, we devised the grating period and width to allow wide range for incident angle.**

Keywords—Si image sensor, metal grating, metal trench, surface plasmon, near-infrared

I. Introduction

Silicon complementary metal-oxide semiconductor (CMOS) image sensors have been applied not only in visible color imaging but also in near-infrared (NIR) imaging such as biological inspection, Time-of-Flight (ToF), surveillance, and fiber optic communication [1-5]. NIR wavelength of 940 nm is mostly used for near-infrared imaging because it is invisible to the human eye and is less affected by sunlight. However, silicon has low absorption efficiency in NIR. Therefore, improving NIR sensitivity is a significant issue for further advancement in NIR imaging technology using silicon CMOS image sensors.

Extending the effective absorption length in a limited thickness of silicon is one of the approaches to improve the sensitivity. It has been reported that silicon pyramid arrays and SiO_2 deep trench isolation (DTI) improved NIR absorption efficiency by the refraction of incident light and repetition of the reflection in silicon layer [6]. Polysilicon nano-grating has been proposed for light confinement in silicon absorption layer with the diffraction [7]. Thus, in recent years, NIR light sensitivity improvement techniques have been actively researched to extend the effective absorption length in silicon.

Our group has proposed silicon-based backside illumination (BSI) image sensor with metal gratings and metal-filled DTI which improved NIR sensitivity by plasmonic diffraction [8,9]. The diffraction efficiency is quite high as ~50% due to the electric field enhancement effect. The diffraction angle was approximately 90 degrees, namely around 80 degrees and the diffracted light was reflected by the metal DTI. Under this large diffraction angle, the effective propagation length dramatically increases in a limited thickness of silicon. Recently, we devised this construction to confine photons in silicon absorption layer, and the absorption efficiency was improved to 53% at an NIR wavelength 940 nm with 3-µm thick of silicon in simulation (Fig. 1) [10,11]. However, this technique is utilized for only normal incidence due to the wave-vector matching conditions of grating. Applying for image sensor pixels, a breakthrough is required to significantly expand the tolerance of the incident angle range. In this paper, we present how to improve the sensitivity with wide incident angles.

II. Near-infrared sensitivity enhancement

A. Plasmonic diffraction

Surface plasmon resonance is excited on a periodic metal grating by light irradiation. The incident photon energy couples with electron oscillation in metal. The resonant oscillation of electrons generates enhanced electric field on the surface of the metal. According to this energy coupling between photons and electrons, the incident light diffracts to horizontal direction, and propagates on the surface of the grating. The resonance wavelength for normal incidence is determined under the matching conditions between the wave vector of surface plasmon and the lattice vector of the metal grating.

We found that the incident light efficiently diffracted to transmission side (silicon side) with a large angle nearly 90 degrees by slightly changing the period of the grating that is corresponding to change the lattice vector. We call this condition quasi-resonance. Fig. 2(a) and Fig. 2(b) show the

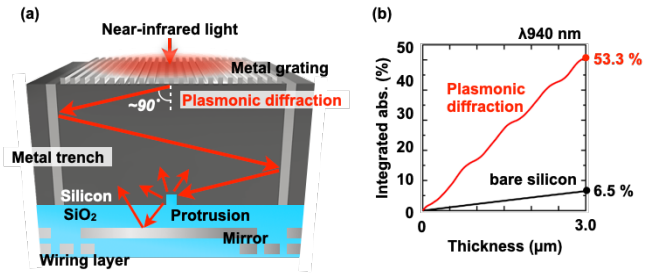

Fig. 1(a) Schematic diagram of the silicon-based image sensor with metal gratings and highly reflective metal DTI. The protrusion scattered photons and the mirror contributed to photon harvesting. (b) Silicon integrated absorption dependence on the silicon thickness [10].

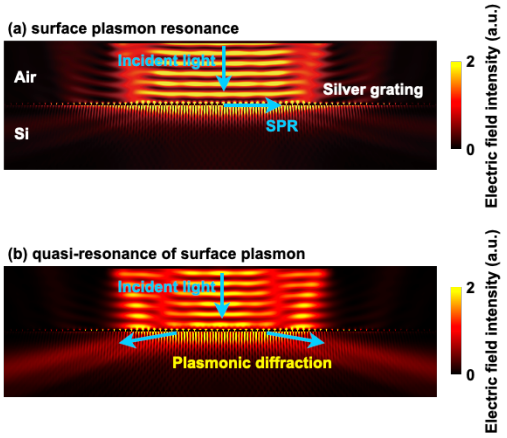

Fig. 2 Electric field intensity distributions in (a) surface plasmon resonance and (b) quasi-resonance of surface plasmon

electric field intensity distributions of a metal grating with the period for surface plasmon resonance condition and for the quasi-resonance condition, respectively. In Fig. 2(a), the incident light from the top excited surface plasmon resonance and the enhanced electric field was observed on the grating. In Fig. 2(b), the incident light diffracted by the grating to the silicon side.

The diffraction angle was about 80 degrees which was extremely high diffraction angle compared with conventional grating. The diffraction efficiency was achieved to ~50% by designing the grating period, width, and height [10-12]. Under the quasi-resonance of surface plasmon, the incident photon energy coupled with the electron oscillation. Re-radiation of the electric dipoles contributed to both high diffraction angle and high diffraction efficiency, that we named "plasmonic diffraction".

B. Near-infrared sensitivity enhancement for Si image sensor

NIR sensitivity was drastically improved by applying the plasmonic diffraction to silicon CMOS image sensor [8-12]. Our proposed construction of image sensor is back-illuminated silicon image sensor pixel with silver grating, silver trench, SiO_2 protrusion, and cupper mirror. Fig. 3 shows the simulation result of electric field intensity distribution. The incident wavelength was set to 940 nm. The structural

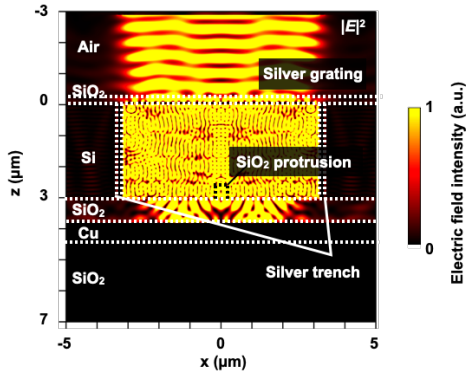

Fig. 3 Simulation result of electric field intensity distribution for photon confinement in silicon absorption pixel using silver grating, silver trench, SiO_2 protrusion, and Cu mirror.

parameters of silver grating were period (p): 265 nm, width (w) 230 nm, and height (h): 85 nm. The plasmonic diffraction light was reflected by the silver trench. The effective absorption length in a limited thickness of 3-μm silicon was extended by confining the photons in silicon absorption layer.

III. Incident Angle Management

Fig. 4 shows the incident angle dependence of the silicon absorption efficiency. The highest absorption efficiency appeared at the incident angle of 0 degree, and the absorption efficiency was drastically dropped over 10 degrees of incidence. Therefore, the incident allowance angle for the proposed image sensor was limited in ±5 degrees. Sensitivity enhancement with wide incident angle is a crucial issue for image sensor with plasmonic diffraction.

The NIR sensitivity for silicon image sensor will be enhanced in the central area of sensor pixels by plasmonic diffraction technique, but the sensitivity will decrease at the area near the edge of sensor because of the angled chief ray. Severe sensitivity enhancement limitation in incident angle is caused by the wave vector matching conditions. From the viewpoint of improving the sensitivity to the angled chief ray, we managed for wide range of incident angles by changing the grating period and width in each pixel toward the edge of the sensor (Fig. 5).

Fig. 6 shows the plasmonic diffraction in each optimized

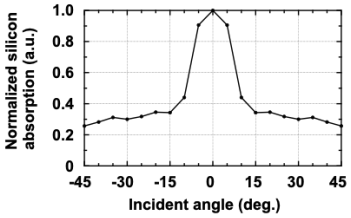

Fig. 4 Simulation result of silicon absorption efficiency dependence on the incident angle.

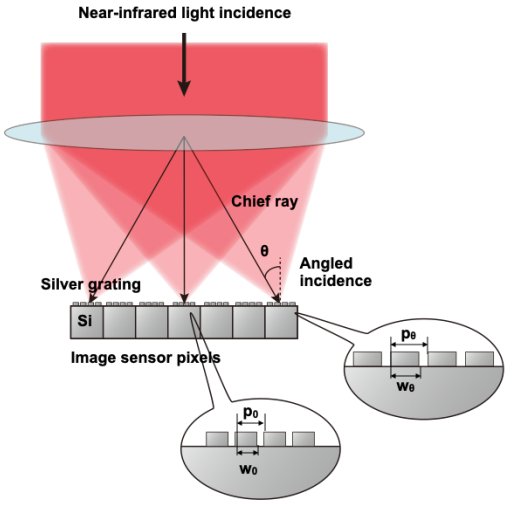

Fig. 5 Schematic image of gradual variation of the period and width of silver grating on silicon image sensor according with angled chief ray incidence. Set (p_0, w_0) and (p_θ, w_θ) were optimized to 0 degree and θ degree incidence, respectively.

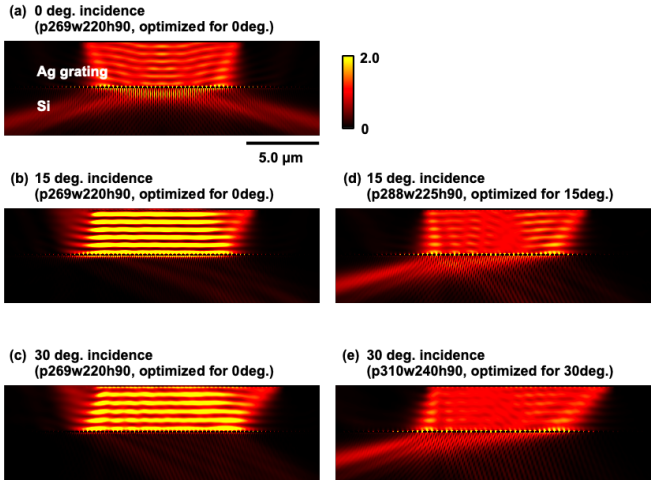

Fig. 6 Simulation results for the plasmonic diffraction with various incident angles. (a)-(c) silver grating was optimized for normal incidence, (d) optimized for 15 degrees of incidence, and (e) optimized for 30 degrees of incidence.

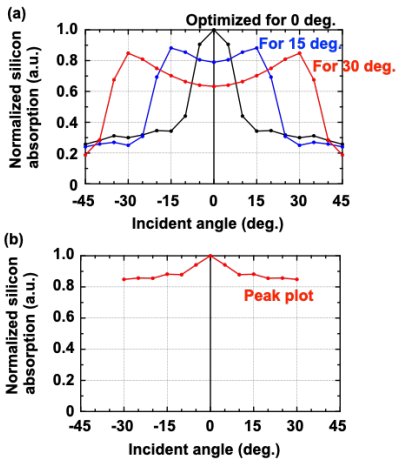

Fig. 7 Simulation results of the normalized silicon absorption efficiency dependence on the incident angle.

parameters for the various incident angles 0, 15, and 30 degrees to keep the absorption efficiencies for wide incident angle. Here, the height of the silver grating was fixed at 90 nm. Although the width and height of the grating will be variable in optimization for each incident angles, it is difficult to change the height in each pixel in the sense of the fabrication process. Lateral patterning parameters such as period and width are easily controlled by mask lithography patterning, but the vertical parameter of height should be the same considering the silver layer formation process. Fig. 6(a)-(c) shows the plasmonic diffraction behavior with parameters of p269 nm, w220 nm, and h90 nm in 0, 15, and 30 degrees of incident angles, which was optimized for 0 degree of incident case. In Fig. 6(a) of normal incidence, incident light diffracted to Si with large diffraction angle. On the other hand, in Fig. 6(b) and 6(c), plasmonic diffraction was not observed and the incident light was reflected back. When the parameters were changed to p288 nm, w225nm, and h90 nm, the angled incident light with 15 degrees diffracted to one side with large diffraction angle. This diffraction will contribute to the absorption enhancement in Si due to the extension of the absorption length (Fig. 6(d)). With the same analogy, the parameters were optimized to p310 nm, w240 nm, and h90 nm for the incident angle at 30 degrees. In Fig. 6(e), the diffraction light was observed in 30 degrees of incident light.

Fig. 7 shows silicon absorption efficiency dependence on the incident angle in each optimized grating parameters. The absorption efficiency was normalized by a peak value at 0 degree of the optimized grating for the normal incidence. In Fig. 7(a), the optimized gratings for 15 and 30 degrees of the incidence exhibited a peak at 15 and 30 degrees, respectively. Fig. 7(b) shows peak plot of the silicon absorption efficiency dependence on the incident angle. By applying each optimized grating parameters for each incident angle, normalized silicon absorption efficiencies were maintained more than 80% in the incident angle range ±30 degrees with 3-μm thick of silicon.

IV. Conclusions

Our proposed silicon-based image sensor with silver gratings and silver filled trench improved NIR sensitivity by plasmonic diffraction which extends the effective absorption length in a limited thickness of silicon. The period, width, and height of silver grating were optimized to efficiently diffracts the incident light with large diffraction angles. Although the incident allowance angles were limited in ±5 degrees because of the wave-vector matching conditions, we clarified that sensitivity improvement by our proposed construction maintained high efficiency between ±30 degrees of incidence by changing the grating period and the width according to each incident angles of chief ray.

Acknowledgment

This research was partially supported by NICT commissioned research (03601) and JSPS KAKENHI (JP22K18984).

References

[1] T. Furukawa, editor, “Biological Imaging and Sensing,” (Springer-Verlag, Berlin, Heidelberg, 2004).

[2] D. Remondinoand and F. Stoppa, “TOF Range-Imaging Cameras,” (Springer-Verlag, Berlin, Heidelberg, 2013).

[3] S. Kawahito, I. A. Halin, T. Ushinaga, T. Sawada, M. Homma, and Y. Maeda, “A CMOS Time-of-Flight Range Image Sensor With Gate-on-Field-Oxide Structure,” IEEE Sens. J. 7(12), 1578-1586 (2007).

[4] Y. Ozaki, C. Huck, S. Tsuchikawa, and S. B. Engelsen, eds. “Near-Infrared Spectroscopy -Theory, Spectral Analysis, Instrumentation, and Applications-,” (Springer Nature Singapore Pte Ltd, 2021).

[5] G. P. Agrawal, “Fiber Optic Communication Systems 4th Ed,” (Wiley-Interscience, 2010).

[6] S. Yokogawa, I. Oshiyama, H. Ikeda, Y. Ebiko, T. Hirao, S. Saito, T. Oinoue, Y. Hagimoto, and H. Iwamoto, “IR sensitivity enhancement of CMOS Image Sensor with diffractive light trapping pixels,” Sci. Rep. 7(1), 3832 (2017).

[7] E. Cobo, S. Massenot, A. L. Roch, F. Corbière, V. Goiffon, P. Magnan, and J.-L. Pelouard, “Design of a CMOS image sensor pixel with embedded polysilicon nano-grating for near-infrared imaging enhancement,” Appl. Opt. 61(4), 960–968 (2022).

[8] A. Ono, K. Hashimoto, and N. Teranishi, “Near-infrared sensitivity improvement by plasmonic diffraction for a silicon image sensor with deep trench isolation filled with highly reflective metal,” Opt. Express 29(14), 21313–21319 (2021).

[9] A. Ono, K. Hashimoto, T. Yoshinaga, and N. Teranishi, “Plasmonic diffraction for the sensitivity enhancement of silicon image sensor,” Proc. IISW, P11 (2021).

[10] T. Yoshinaga, K. Hashimoto, N. Teranishi, and A. Ono, “Photon confinement in a silicon cavity of an image sensor by plasmonic diffraction for near-infrared absorption enhancement,” Opt. Express 30(20), 35516-35525 (2022).

[11] T. Yoshinaga, K. Hashimoto, N. Teranishi, and A. Ono, “Near-Infrared Sensitivity Enhancement of Silicon Image Sensor by Photon Confinement with Plasmonic Diffraction,” SSDM, G-5-05 (Late News), 523-524 (2022).

[12] N. Teranishi, T. Yoshinaga, K. Hashimoto, and A. Ono, “Near-Infrared Sensitivity Enhancement of Image Sensor by 2nd-Order Plasmonic Diffraction and the Concept of Resonant-Chamber-Like Pixel,” IEDM, 37.2 (2022).